# Dimensional Stability of 3D Printed Parts: Effects of Process Parameters

ELIZABETH AZHIKANNICKAL[1]; AARON UHRIN, Muskingum University, New Concord, OH, USA.

ABSTRACT. The three-dimensional (3D) printing manufacturing process begins with the creation of a 3D model—using computer aided design (CAD) software—of the part to be printed. Using a type of 3D printing known as fused deposition modeling (FDM®), the 3D printer extrudes molten plastic to scan lines to create individual layers (i.e., the infill): one on top of the other. (Note that "scan" in this context refers to the movement of the extruder head, along an x,y coordinate path, while depositing molten plastic.) This process is repeated until the overall geometry, specified by the 3D model, is built. This process is attractive for producing proof of concept or prototype parts in various fields including automotive, aerospace, and medical. However, FDM subjects the material to rapid heating and cooling; therefore, some degree of undesirable warpage of the part occurs post fabrication. The primary objective of this study was to determine the effect of 4 process parameters (i.e., infill shape, infill density, number of perimeters created per layer, and layer height) on the total dimensional error of a representative 3D-printed part. This part (the "simple part"), used in Trials 1 through 3 of this study, was a square acrylonitrile butadiene styrene (ABS) plate having a nominal measurement of 50 mm × 50 mm × 5 mm thick. A residual error (the difference between the measured post-printing dimension and the theoretical CAD file dimension) was calculated along each given direction and for each test print. Finally, a root mean square (RMS) error (i.e., the square root of the average of the squared residual errors along the length, width, and thickness directions) was calculated for each printed part. Three repeat test prints were carried out for each parameter. The number of perimeters played a key role in the dimensional stability of the part. As the number of perimeters increased up to 5, the RMS error decreased. Beyond 5 perimeters, however, the RMS error increased due to excessive warpage/curvature at the corners of the part. Ultimately, when examined individually, a grid infill shape at 100% density, a 0.4 mm layer height, and 5 perimeters each produced the lowest warpage. In combination, these same 4 parameters also produced the lowest RMS error (based on dimensional analysis of 3 test prints) when used to print a more complicated part (the "stacked part") in Trial 4.

## INTRODUCTION

*The purpose of this study was to examine the effects of 4 specific 3D printing process parameters on the dimensional stability of a printed part: comparing the dimensions of the final part to the originally input computer aided design (CAD) geometry. The goal was to determine an optimal set of printing parameters, which would result in the least warpage of a final printed part as compared to the input 3D geometry.*

Three-dimensional (3D) printing is an additive manufacturing (AM) process patented in the early 1990s (Chandler 2011). In this process, a digital 3D model of a part is first created using CAD software or reverse engineered by 3D scanning. The 3D model is then loaded into printer-compatible software to facilitate manufacturing. This software (i.e., Simplify3D®) is used to set the process parameters and then slice the model into layers for printing. The sliced file is typically opened with the printer and the printing process initiated. Utilizing the fused deposition modeling (FDM®) process, the 3D printer extrudes molten plastic to scan lines to create the individual layers of the part. Once an individual layer is created, the next layer is constructed on top using an additional sequence of scanned lines. This process is repeated until the entire part is built.

Various industry sectors—including aerospace, automotive, architecture, healthcare, and robotics—use 3D printing to create components of interest. The ability of 3D printing to decrease weight (i.e., through the creation of internal honeycomb-style structures) is particularly attractive for the automotive industry (Gardan et al. 2015). Another trend in AM

[1]Address correspondence to Dr. Elizabeth Azhikannickal. Email: azhikae@gmail.com

is bioprinting, which has the potential to create tissues and organs at hospitals as well as the construction of prosthetics for biomedical uses (Dean et al. 2003).

One of the major advantages of the AM process is prototyping—its capability to create very intricate parts to demonstrate and validate their functionality, aesthetics, engineering properties, etc. Often the AM process can produce components that would be difficult and/or cost prohibitive to make using conventional manufacturing processes (e.g., milling or injection molding) or that would be difficult to produce on a small scale (to serve as a proof of concept). Parts with intricate geometries, asymmetrical features, and/or unique curved surfaces can be more easily and inexpensively produced through the AM process. In addition, common issues such as component release from a mold (after the production of a complicated part) are not a barrier for the AM process. The AM process also provides the potential for replicating parts that are no longer produced or no longer available commercially.

A few of the drawbacks of the 3D printing process are reduced dimensional stability of the final printed part, limited strength and/or toughness of the resulting part, and the potential for long print times for complex parts.

Building printed components with adequate dimensional stability is important, especially where these parts are mated or integrated into larger mechanical assemblies. The main obstacle is the distortion of the final product when 3D printing is used to construct these larger parts (Hwang et al. 2015). This is partially due to the increased potential for warpage, because the part undergoes repeated heating and cooling cycles during construction. Even with the use of a heated stage, only the layer(s) closest to the stage will be maintained at a constant temperature. The greater the height of the part, the greater the potential for asymmetrical temperature profiles through the part.

Much of the existing research centers on the use of 3D printing to create parts with enhanced mechanical properties (Maurath and Willenbacher 2017; Al-Qutaifi et al. 2018; Kuznetsov et al. 2018). However, fewer studies have comprehensively quantified the effects of various printing process parameters, acting individually and in combination, on the dimensional stability of the final part (Ippolito et al. 1995; Dimitrov, Schreve, et al. 2006; Dimitrov, van Wijck, et al. 2006; Mantada et al. 2017; Rajamani

et al. 2018). In a recent study, Dixit et al. (2016) examined the effect of raster width, slice height, and path speed on the FDM process. They employed the grey relational method to obtain an optimal parameter level for each dimension studied simultaneously. The effect of parameters such as infill shape and density on part dimensional stability was not explored.

In another study, Islam et al. (2013) provided experimental results of a preliminary study of the dimensional accuracy of parts produced by 3D printing. The part was a 50 mm × 50 mm × 50 mm U-shaped channel with a hole at the bottom of the U shape. A coordinate measuring machine (CMM) was used to determine the dimensional change of the part, both in terms of variation of linear dimensions and hole dimensions. The results of the study indicated that the maximum variation in the length, width, and hole diameter was 0.2 mm based on a single set of printing conditions. The effect of changing process conditions was not examined in this study.

## METHODS AND MATERIALS
### Printer, Test Part, and Test Parameters

This research used a Bits from Bytes 3D Touch printer. This printer has a 275 mm × 275 mm × 210 mm build volume, an unheated build plate (or stage), and dual 0.35 mm nozzle extruders. It is housed in the Department of Physics and Engineering at Muskingum University, and is used for undergraduate teaching and research purposes. Simplify3D was used to specify the printing process parameters (i.e., infill shape, scan speed, etc.). The process file was created in Simplify3D, then saved as a BFB file which could be read by the 3D printer in order to fabricate the part. The samples in this study were printed from acrylonitrile butadiene styrene (ABS) material.

The representative part (used in Trials 1 through 3, of the 4 total trials) was a square ABS plate measuring 50 mm × 50 mm with a thickness of 5 mm—hereafter referred to as the "simple part." This same plate design was used to measure the variations in length, width, and thickness resulting from each of the different process conditions studied. It was decided that a simple geometry would be better, as dimensional changes would be easier to quantify compared to samples with curved sections and/or holes.

The specific parameters examined were infill shape (i.e., diagonal scan pattern and grid scan pattern), infill density (i.e., 20%, 50%, and 100%), number

of perimeters used to create each printed layer, and layer height. The infill shape refers to the pattern created by the molten plastic as it fills in each layer of the part. The infill density refers to how densely each layer is filled in using a given scan pattern. The number of perimeters refers to the number of times the printer traverses the outer border of the part before printing the infill for a given layer. The layer height refers to the amount that the stage would move down, after creating a given layer, before the next layer was scanned.

The scan speed (2,000 mm/min) and print temperature (230 °C) parameters were kept constant for all trials. The scan speed was selected as it lay in the middle of the range of scanning speeds available for the printer. No external cooling was used during printing, permitting insight into the material's inherent behavior (i.e., warpage) after printing. Finally—and in order to understand and quantify inherent material warpage (in the form of corner uplifting, thinning, etc.) resulting from specific process parameters—no support structures (i.e., rafts) were used.

Once printing was complete, the sample cooled to room temperature. At this point, measurements of the length, width, and thickness of the sample were taken using a Mitutoyo® caliper. Typically, 3 repeat prints were carried out for each parameter being studied.

The RMS error was calculated using this equation:

$$RMS\ error = \sqrt{\frac{\sum_i^n[(l_{mi} - l_{ti})^2 + (w_{mi} - w_{ti})^2 + (t_{mi} - t_{ti})^2]}{3n}}$$

where $l_{mi}$ is the measured length for test print $i$, $l_{ti}$ is the theoretical length (from the CAD geometry) for test print $i$, $w_{mi}$ is the measured width for test print $i$, $w_{ti}$ is the theoretical width (from the CAD geometry) for test print $i$, $t_{mi}$ is the measured thickness for test print $i$, $t_{ti}$ is the theoretical thickness (from the CAD geometry) for test print $i$, and $n$ is the number of test prints.

## Trials 1 to 4

Trial 1 examined the effect of infill shape and infill density on the simple part's dimensional stability. The printer was set to a layer height of 0.2 mm. The 2 infill shapes studied were a diagonal scan pattern and a grid scan pattern; the 3 infill densities studied were 20%, 50%, and 100%. In each case, each layer was created by first having the printer scan 2 full perimeters which created the outside boundaries of the part (Fig. 1a). After creating the perimeters, the part was printed using the selected infill pattern and infill density. This process was repeated until the part was built up to the correct height (i.e., 5 mm) as stipulated in the CAD file. Fig. 1a and Fig. 1b show the creation of a single layer for the diagonal and grid scan patterns, respectively.

Trial 2 examined the effect of the number of perimeters, created in each individual layer, on the dimensional stability of the simple part. The infill shape and density were based on the results from Trial 1 (the shape and density combination resulting in the lowest RMS error). Prints were conducted with 0, 2, 5, 7, and 10 perimeters. The number of perimeters affected the uniformity of the thickness profile: along both the length and width edges. For this reason, and for each perimeter case, thickness measurements were taken at equally spaced locations along the edge of the sample. Specifically, measurements were taken at 0, 12.5 mm, 25 mm, 37.5 mm, and 50 mm along the edge. These additional profile measurements provided greater insight into the asymmetric nature of the warpage—both in terms of the RMS error and thickness profile evolution—as a function of the number of perimeters used.

Trial 3 examined the effect of layer height on the dimensional stability of the simple part. The infill shape and density were based on the results from Trial 1 (the shape and density combination resulting in the lowest RMS error). The number of perimeters used was based on the results of Trial 2 (the number of perimeters resulting in the lowest RMS error). The layer heights tested were 0.1 mm, 0.2 mm, 0.33 mm, and 0.4 mm.

Trial 4 used the optimized parameters obtained from Trials 1 to 3 to print a slightly more complicated part—hereafter referred to as the "stacked part"—shown in Fig. 2. RMS errors were subsequently calculated on this part. The stacked part was designed using CAD software and was comprised of 3 simple geometric shapes: a hexagon measuring 50 mm between opposite sides, a 50 mm diameter circle, and a 30 mm wide × 30 mm long square. Each tier was 10 mm thick and stacked one on top of the other. Each dimension of each shape was measured and compared to the theoretical dimensions from the CAD file (i.e., a residual error was calculated) and the RMS error was calculated based on the residual errors.
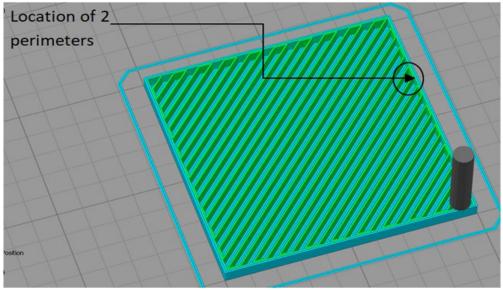
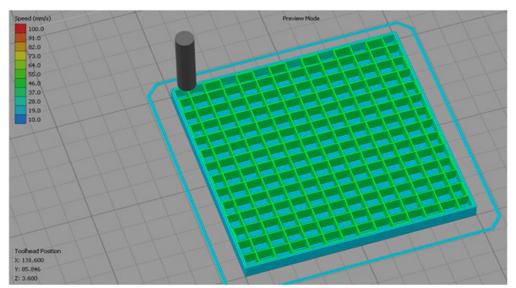**FIGURE 1a. Schematic of diagonal scan pattern**
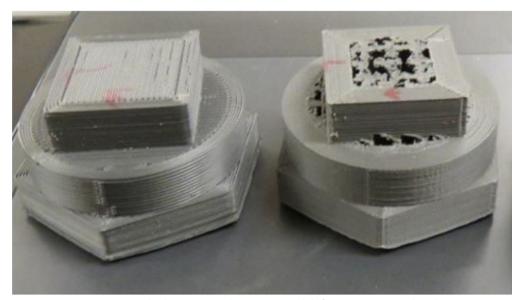


**FIGURE 1b. Schematic of grid scan pattern**



**FIGURE 2. Stacked part printed using optimal (left) vs. non-optimal (right) process parameters to examine effects on dimensional stability**

## RESULTS

### Trial 1

Fig. 3 shows the effect of infill shape and infill density on the RMS error. For the grid scan pattern, Fig. 3 indicates that the RMS error decreases with increasing infill density. For the diagonal scan pattern, the RMS error increases slightly from 20% to 50% infill density and then decreases from 50% to 100% infill density. Based on these results, the infill shape parameter had a larger effect on part warpage; the infill density parameter had a smaller effect on part warpage. The grid pattern at 100% infill density produced the lowest RMS error; therefor, this combination of infill shape and infill density were used in all subsequent experiments.

### Trial 2

A grid pattern at 100% infill density (the combination resulting in the lowest RMS error from Trial 1) was used for Trial 2. Fig. 4 shows the effect of the number of perimeters on the errors (i.e., difference between measured value and theoretical CAD dimension) along the length, width, and thickness directions as well as on the RMS error. Fig. 4 shows that as the number of perimeters increases from 0 to 7, the error along the length and width directions continues to decrease. Beyond 7 perimeters, the error along the length and width increases. Along the thickness direction, however, the error decreases from 0 to 2 perimeters, but increases beyond 2 perimeters. The RMS error decreases from 0 to 5 perimeters, but increases beyond 5 perimeters. These data indicate that progressing from 0 up to 5 perimeters work to restrict the RMS error of the part. Beyond 5 perimeters the RMS error begins to increase, indicating that a competing material effect is contributing to the increased RMS error.

Visual examination revealed that samples containing more than 5 perimeters exhibited a greater uplift in the corners. This feature, as expected, appeared to have the greatest impact on the warpage along the thickness direction, thereby contributing to the larger RMS error (beyond 5 perimeters). Fig. 5 shows how the edge thickness of the sample varies with position along the length direction. As indicated in this figure, the 10-perimeter case produced a sample with thinner sections at the corners of the sample compared with the 0-perimeter case. This is due to the excessive uplift of the corners resulting in increased thinning of the material at these locations.

Fig. 6 shows the curvature of actual samples, ranging from 0 perimeters to 10 perimeters. This figure shows the notably increased corner uplift of the sample when greater than 5 perimeters were used, resulting in the increased RMS error at 7 and 10 perimeters. Using 5 perimeters appeared optimal between achieving the lowest RMS error and a relatively uniform thickness profile.
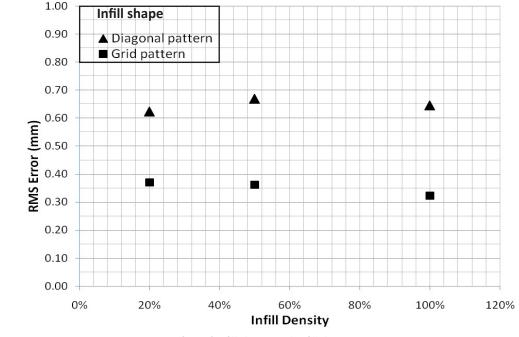


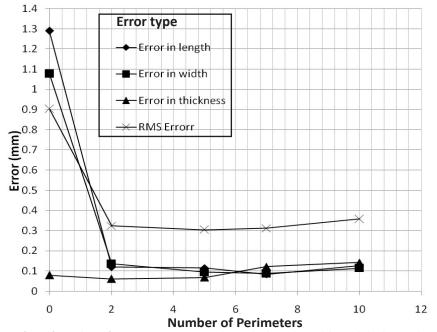FIGURE 3. Effect of infill shape and infill density on RMS error

**FIGURE 4. Effect of number of perimeters on error along the length, width, and thickness directions, and RMS error**
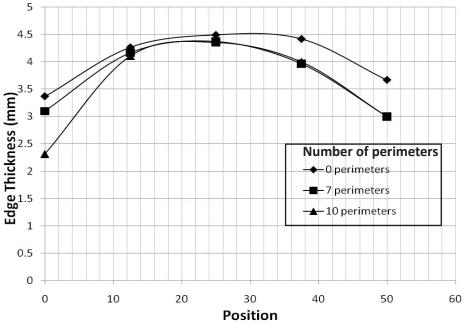


**FIGURE 5. Sample thickness measurements corresponding to 0, 7, and 10 perimeters**



**FIGURE 6. Sample thickness profiles corresponding to 0, 2, 5, 7, and 10 perimeters**

## Trial 3

Based on the results from Trial 1 and 2, a grid pattern with 100% infill density and 5 perimeters was used for Trial 3 (i.e., examining the effect of layer height). Fig. 7 shows the effect of layer height on the RMS error. As indicated in this figure, as the layer height increases the RMS error decreases. However, when layer heights larger than 0.4 mm were tested, all the prints failed to adhere to the print surface (and failed to remain within the boundaries of the part). At larger layer heights (i.e., greater than 0.4 mm) the molten plastic leaving the nozzle had to fall a greater distance, resulting in a less controlled deposition of the plastic on the previous layer. A 0.4 mm layer height appeared optimal.

## Trial 4

Trial 4 required the printing of 2 separate samples of the stacked part. The first stacked part used the optimal parameters obtained from Trials 1 through 3; the second stacked part used a set of non-optimal parameters. These 2 parts were compared. The optimal parameters used for this test were: grid pattern, 100% infill, 5 perimeters, and 0.4 mm layer height. The non-optimal parameters used were: grid, 20% infill, 10 perimeters, and 0.1 mm layer height.

The stacked part produced using the optimal parameters exhibited a lower RMS error, totaling 0.14 mm. The non-optimal parameters produced a part with an RMS error close to 2.5 times greater than the optimal case.
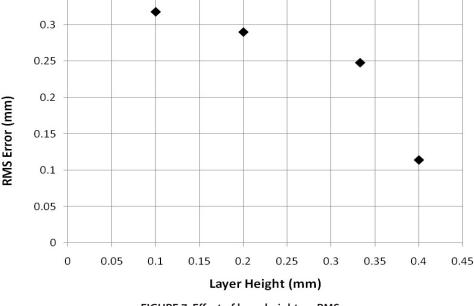
## DISCUSSION

This study examined the effect of 4 specific printing process parameters—infill shape, infill density, number of perimeters, and layer height—on the dimensional stability of 3D printed parts. Based on the results of this study, it was determined that a grid scan pattern at 100% infill density produced the lowest total RMS error.

Perimeters, when used in the proper number, contributed to restricting overall part warpage. Printing using no perimeters resulted in the largest RMS error; however, as the number of perimeters increased up to 5, the RMS error decreased. Using 5 perimeters appeared optimal. Visual examination of the samples containing more than 5 perimeters revealed that the corners exhibited a greater uplift and a much more non-uniform thickness profile. Above 5 perimeters, these additional factors contributed to a larger error along the thickness direction and subsequently contributed to a larger RMS error.

Finally, as layer height increased the RMS error decreased—up to an optimal layer thickness of 0.4 mm. Beyond 0.4 mm, the prints failed to adhere to the print bed and the molten plastic scattered in random directions.

When applied to the stacked part this same combination of 4 optimal parameters also resulted in a lower RMS error, compared with this same part printed using a set of non-optimal parameters.



FIGURE 7. Effect of layer height on RMS error

***In summary, the printing parameters that resulted in the lowest RMS error (the least warpage) were: a grid-pattern infill shape, a 100% infill density, a 0.4 mm layer height, and 5 perimeters.***

The results of this study provided greater insight into how process parameters can be set/controlled to minimize component warpage, especially with FDM printers that have similar temperature control.

In the future, this study could be expanded to examine the effects of additional process parameters (e.g., scan speed, temperature, material, use of a heated stage, etc.) on warpage. It would also be valuable to assess the impact of these additional parameters, individually or in combination, on parts of varying geometry and overall size. Such a comprehensive study would aid in confirming that a set of optimal printing parameters are, in fact, independent of component geometry. These optimal printing parameters could be implemented as guidelines in the 3D printing process, particularly if further validation was conducted with different FDM printers as well as other types of printers.

## ACKNOWLEDGMENTS

## LITERATURE CITED

Al-Qutaifi S, Nazari A, Bagheri A. 2018. Mechanical properties of layered geopolymer structures applicable in concrete 3D-printing. Constr Build Mater. 176:690-699. https://doi.org/10.1016/j.conbuildmat.2018.04.195

Chandler DL. 2011. Printing off the paper: MIT research continues to push the boundaries of the burgeoning technology of 3-D printing. MIT News. [published 2011 Sep 14; accessed 2019 Jun 2]. http://news.mit.edu/2011/3d-printing-0914

Dean D, Min KJ, Bond A. 2003. Computer aided design of large-format prefabricated cranial plates. J Craniofac Surg. 14(6):819-832. https://doi.org/10.1097/00001665-200311000-00002

Dimitrov D, Schreve K, de Beer N. 2006. Advances in three-dimensional printing - state of the art and future perspectives. Rapid Prototyping J. 12(3):136–147. https://doi.org/10.1108/13552540610670717

Dimitrov D, van Wijck W, Schreve K, de Beer N. 2006. Investigating the achievable accuracy of three dimensional printing. Rapid Prototyping J. 12(1):42–52. https://doi.org/10.1108/13552540610637264

Dixit NK, Srivastava R, Narain R. 2016. Dimensional accuracy improvement of part fabricated by low cost 3D open source printer for industrial application. Proceedings of the 10th International Conference on Intelligent Systems and Control (ISCO); 2016 Jan 7-8; Coimbatore (India). IEEE. p. 1-6. https://doi.org/10.1109/ISCO.2016.7726882

Gardan N, Schneider A, Gardan J. 2015. Material and process characterization for coupling topological optimization to additive manufacturing. Comput Aided Design Appl. 13(1): 39-49. https://doi.org/10.1080/16864360.2015.1059192

Hwang S, Reyes EI, Moon KS, Rumpf RC, Kim NS. 2015. Thermo-mechanical characterization of metal/polymer composite filaments and printing parameter study for fused deposition modeling in the 3D printing process. J Electron Mater. 44(3):771-777. https://doi.org/10.1007/s11664-014-3425-6

Ippolito R, Iuliano L, Gatto A. 1995. Benchmarking of rapid prototyping techniques in terms of dimensional accuracy and surface finish. CIRP Ann-Manuf Techn. 44(1):157–160. https://doi.org/10.1016/S0007-8506(07)62296-3

Islam MN, Boswell B, Pramanik A. 2013. An investigation of dimensional accuracy of parts produced by three-dimensional printing. Proceedings of the World Congress on Engineering 2013 Vol I; 2013 July 3-5; London (UK). International Association of Engineers. p. 522-525. http://www.iaeng.org/publication/WCE2013/WCE2013_pp522-525.pdf

Kuznetsov VE, Solonin AN, Urzhumtsev OD, Schilling R, Tavitov AG. 2018. Strength of PLA components fabricated with fused deposition technology using a desktop 3D printer as a function of geometrical parameters of the process. Polymers-Basel. 10(3):313-323. https://doi.org/10.3390/polym10030313

Mantada P, Mendricky R, Safka J. 2017. Parameters influencing the precision of various 3D printing technologies. Mod Mach Sci J. December 2017:2004-2012. https://doi.org/10.17973/MMSJ.2017_12_201776

Maurath J, Willenbacher N. 2017. 3D printing of open-porous cellular ceramics with high specific strength. J Eur Ceram Soc. 37(15):4833-4842. https://doi.org/10.1016/j.jeurceramsoc.2017.06.001

Rajamani D, Balasubramanian E, Arunkumar P, Silambarasan M, Bhuvaneshwaran G. 2018. Experimental investigations and parametric optimization of process parameters on shrinkage characteristics of selective inhibition sintered high density polyethylene parts. Exp Techniques. 42(6):631-644. https://doi.org/10.1007/s40799-018-0286-6